PtZn-ETS-2: A Novel Catalyst for Ethane Dehydrogenation

Zhengnan Yu, James A. Sawada, Weizhu An, and Steven M. Kuznicki
Dept. of Chemical and Materials Engineering, University of Alberta, Edmonton, AB, Canada T6G 2V4

DOI 10.1002/aic.15010
Published online August 25, 2015 in Wiley Online Library (wileyonlinelibrary.com)

Catalysts having unprecedented selectivity toward ethane dehydrogentation were prepared by combining platinum and zinc on the surface of the titanate ETS-2. This high surface area, sodium titanate ion exchanger affords high metal dispersion, presents many active sites to the gas stream, and is free of any pore structure that can influence mass transfer to and away from the active sites. It was determined that the addition of zinc to platinum-loaded ETS-2 changes the electronic properties of the metals and significantly improves the specificity of the catalyst. By changing the zinc-to-platinum ratio, and by manipulating the space velocity of the gas, the production of side products and coke can be suppressed or eliminated. © 2015 American Institute of Chemical Engineers *AIChE J*, 61: 4367–4376, 2015
Keywords: ethane dehydrogenation, ethylene, catalyst, platinum, ETS-2

Introduction

Ethylene is an important precursor for the petrochemical industry. The global ethylene capacity is projected to reach over 170 million tons in 2016 by growing at a rate of 3.4% per year.[1] Ethylene is typically manufactured by steam cracking a hydrocarbon feedstock. Currently, ethane and naphtha are the two main feedstocks for ethylene production but ethylene production from ethane is the more economical[2] and efficient due to the abundant reserves, easy exploitation of natural gas, and the higher selectivity of the cracking process. Using ethane as the feedstock, conversion can be up to 70% with olefin yields of around 52%. By contrast, using naptha as a feedstock the ethylene yield is typically around 28%.[3]

Catalytic dehydrogenation of ethane has been an attractive alternative to steam cracking because the lower reaction temperature afforded by catalysis reduces the energy required for ethylene production. Supported platinum catalysts have been investigated for ethane dehydrogenation[4–9] and it was proved that acidic supports such as Al_2O_3 and MFI zeolites helped the dispersion and stabilization of the active metal phase. However, the acid function of the supports simultaneously catalyzed undesired reactions such as polymerization and coking,[10,11] which converted the ethylene product into low-value by-products. As a result, nonacidic supports, such as potassium modified L-zeolite,[12] hydrotalcites,[5,7,8,13–16] alkali modified Al_2O_3,[17–20] and spinels[21,22] were studied to overcome this disadvantage. Previous studies showed that alkaline supports helped reduce, but did not eliminate, the formation of coke.

Further enhancements in catalyst selectivity were realized using bimetallic catalyst systems. Since the 1960s bimetallic catalyst systems including platinum were developed to improve the selectivity of cracking catalysts. For alkane dehydrogenation, adding a second metal component to the catalyst was found to generate higher stability and alkene selectivity. Tin was widely investigated as a promoter for Pt-based catalysts.[6,7,9,12,21–29] During the catalyst reduction processes, Pt and Sn formed Pt-Sn alloys[6,30] on the surface of the support. The Sn in Pt-Sn alloy reduced the Pt into nanoparticulate sizes[12,24] and the addition of Sn changed the geometric structure and electronic properties of the Pt particles[21]; weakening the interaction of propene with Pt on the PtSn-Al_2O_3 catalyst. These effects combined to achieve a higher propane conversion,[24] decreased coke deposit on the catalyst surface,[7,9,24,26] increased catalyst stability,[21] and eliminated the acid sites on the supports.[22] While the addition of Sn significantly improved catalyst performance, the bimetallic catalyst is not completely selective toward ethane as ethane, ethylene, and hydrogen all compete for the same adsorption sites.[5] Isotopic tracer studies[5,7] demonstrated that methane was generated—not through reaction with ethane—but by ethylene dehydrogenation. Preventing ethylene adsorption on the catalyst sites is critical to further improving catalyst selectivity.

Zinc has also been used as a promoter or as a composite support for alkane dehydrogenation catalysts.[31–35] Zinc, analogously to tin, modifies the geometric and electronic properties of the metallic phase of Pt and studies showed that the addition of zinc to Pt-Al_2O_3, PtSn-Al_2O_3,[31] and PtSn-$MgAl_2O_4$ formulations significantly improved their overall performance for propane dehydrogenation.[33] ZnO-supported Pt catalysts were found to have increased Pt dispersion and reduced metal particles sizes on the surface of the support. The mechanism behind this improvement is believed to lie in the way in which the metals interact.

Zinc is known to alloy with platinum and the formation of the alloy increases the electronic density on the metallic Pt. The enriched electron density of Pt weakens the adsorption strength of ethylene (π-bonded) on Pt surface[31] which, in turn, suppresses coke formation and associated by-product gases such as methane.[36] The addition of ZnO was shown to improve the activity and stability of a PtSn-$MgAl_2O_4$

Correspondence concerning this article should be addressed to S. M. Kuznicki at steve.kuznicki@ualberta.ca.

catalyst.[33] However, pure ZnO-supported Pt catalyst (PtZnO) was less active than the compound oxides supported Pt ($PtZnO\text{-}M_2O_3$) for *i*-butane dehydrogenation.[37,38]

In this work, a novel bimetallic catalyst supported on the titanate ETS-2 was developed and characterized for its selectivity toward ethane dehydrogenation. ETS-2 was first introduced by Kuznicki[39] as a high surface area sodium titanate. ETS-2 is formed by the alkaline digestion of TiO_2 and the caustic digestion converts the surface of the TiO_2 particles into sodium titanate which is a potent ion-exchanger; particularly for transition metals which makes it particularly suitable as a metal support. The core of the ETS-2 particles is presumed to be TiO_2 while the surface titanate species carry a net negative charge, which is offset by exchangeable cations. ETS-2 has no measurable microporosity—which makes it immune to pore blockage or capillary condensation—yet has a surface area as high as 250 m^2/g, which exposes a large number of active sites to a gas stream. The effect of the Zn content on the specificity of the PtZn-ETS-2 catalysts toward the ethane dehydrogenation reaction was investigated, as was the influence of the space velocity of the feed gas stream on ethane conversion and ethylene selectivity.

Experimental

Catalyst preparation

A commercial ETS-2 sample in the form of filter cake was received and used to prepare the catalysts. The filter cake was calcined at 600°C for 4 h and crushed into 30–50 mesh pellets to be used as the catalyst support. A series of PtZn-ETS-2 catalysts having varying zinc loadings was prepared by impregnating the pellets with the metals via the incipient wetness impregnation method.

Metal precursors were prepared from aqueous solutions: 0.1 M H_2PtCl_6 (Hydrogen hexachloroplatinate (IV) hydrate, Pt 40%, Acros Organics), 0.2 M $Zn(NO_3)_2$ (Zinc nitrate hexahydrate crystalline, Fisher Scientific, Canada). The ETS-2 granules were first modified with Zn to the target loading and then impregnated with 1 wt % Pt. All catalysts were calcined at 500°C in air for 4 h except for where specified.

Catalyst characterization

X-ray Diffraction. The phase identification and structural analysis of the catalyst materials was carried out using powder x-ray diffraction (XRD) on a Rigaku Gigerflex 2173 diffractometer having a Co tube x-ray source (Co Kα, $\lambda = 1.79021$ Å), and a vertical goniometer with a graphite monochromator as Kβ filter. Testing conditions were: 38 kV, 38 mA, scan speed 2°/min, step width 0.02°, and scan range 5–90° (2θ).

Specific Surface Area (Brunauer–Emmett–Teller). The influence of the calcination process and metal impregnation on the surface area of the titanate particles was measured using N_2 physisorption. The specific surface areas of the samples were calculated using the Brunauer–Emmett–Teller (BET) method from the N_2 adsorption isotherm using a Micrometrics ASAP 2020C instrument. Samples were degased at 200°C for 4 h before adsorption.

X-ray Photoelectron Spectroscopy. X-ray photoelectron spectroscopy (XPS) measurements were carried out to identify the oxidation state of the Zn and Pt metals on the surface of the titanate. XPS spectra were collected using a Kratos Axis 165 x-ray photoelectron spectrometer with a Mono Al Kα source ($h\nu = 1486.6$ eV) (operated at 15 mA and 14 kV). The survey spectra were collected with analyzer pass energy of 160 eV and a step of 0.4 eV; the high resolution spectra were scanned with a pass energy of 20 eV and a step of 0.1 eV. During the acquisition of a spectrum, charge neutralization was applied to compensate the insulating problem of the sample. XPS signals were fitted by mixed Lorentzian–Gaussian curves using Casa XPS software. All binding energies are reported after calibration for C1s peak to match 284.8 eV.

Temperature-Programmed Reduction. Temperature-programmed reduction (TPR) measurements were carried out to differentiate the reduction behaviors of the various catalyst compositions. Hydrogen temperature-programmed reduction (H_2-TPR) was carried out on an AutoChem 2950 HP instrument (Micromeritics) equipped with thermal conductivity detector under atmospheric pressure. About 0.5 g of the catalyst was calcined in air, at 200°C, for 1 h, and used for the analysis. The catalysts were reduced in a flow of 10% H_2/Ar (50 mL/min) from room temperature to 500°C with a heating rate of 5°C/min.

Scanning Electron Microscopy and Energy Dispersive X-ray. Particle morphology and Pt dispersion was assessed using electron microscopy. The scanning electron microscopy (SEM) images were analyzed by a Hitachi S-2700 scanning electron microscope equipped with a PGT (Princeton Gamma-Tech) IMIX digital imaging system and a PGT PRISM IG (Intrinsic Germanium) detector for energy dispersive x-ray (EDX) analysis. Samples for EDX were coated with carbon.

Thermal Gravimetry-Mass Spectrometry. The analysis of coke deposits on the spent catalysts was carried out using thermal gravimetry-mass spectrometry (TG-MS). The TG-MS plots were collected using a TA Instruments Q500 TGA coupled to a Pfeiffer Omnistar QMA 200 residual gas analyzer. TG scans were run using a balance purge rate of 5 mL/min Ar and a sample (air) purge rate of 180 mL/min. Samples were loaded on platinum pans and heated at a rate of 10°C/min from ambient to 600°C.

The mass spectrometer was configured with a stainless steel capillary heated to 200°C and connected to the TGA by means of a stainless steel adapter and a 0.25″ branch T-fitting. The capillary was positioned at the center of the tee close to the furnace exhaust to sample the evolved gases. The exhaust end of the T-fitting was connected to a 6 m length of 0.25″ OD tubing that prevented back-diffusion of atmospheric components and led to a fume hood exhaust. Experiments were run in MID mode with fragments at $m/z = 18$ and 44 tracked over time. These fragments, associated with water and carbon dioxide, respectively, were found to be the most diagnostic signals associated with the combustion of the coke. To start data collection, the two instruments were manually synchronized and, as a result, an uncertainty of a few tenths of a degree for the starting temperature can be expected between the TG and MS plots.

Catalysts testing in ethane dehydrogenation reaction

To evaluate the catalyst performance for the ethane dehydrogenation reaction, a reactor as shown in Figure 1 was configured. The reactor was a quartz tube (ID 22 mm) and the catalyst bed was supported by quartz wool on both sides. Both reduced and nonreduced catalysts were dried at 110°C for 4 h before use. The catalysts were reduced *in situ* using 40 mL/min of argon-diluted hydrogen (40 vol % H_2) and at a rate of 2°C/min from room temperature to 300°C. Samples were maintained at 300°C for 1 h.

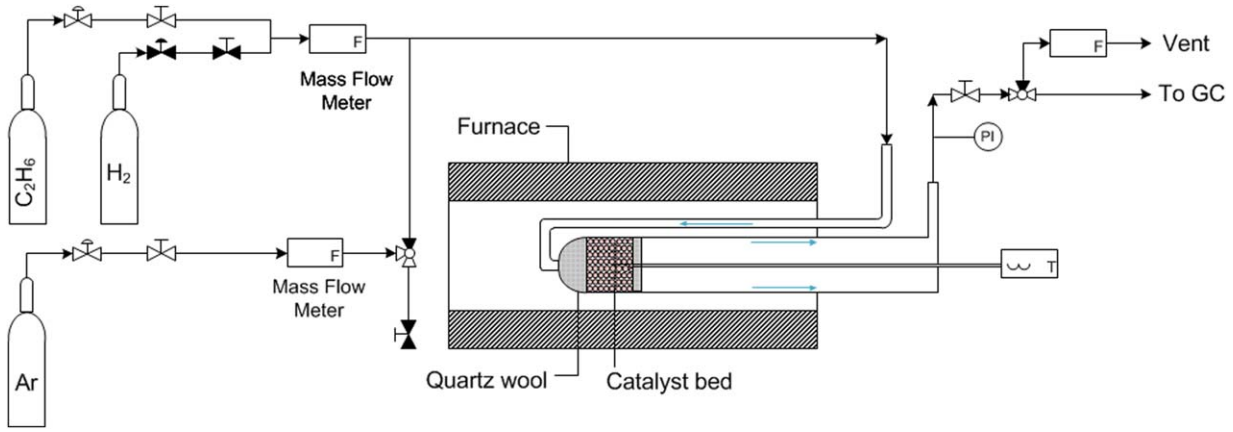

Figure 1. The scheme of packed-bed reactor for ethane dehydrogenation.

[Color figure can be viewed in the online issue, which is available at wileyonlinelibrary.com.]

The amount of the catalyst loaded for each run was 3.0 g. An online GC (Bruker 450-GC) was used to analyze the gas products. The ethane feed (99.5%, Praxair) flow rate was controlled by a mass flow meter (Sierra Instruments). The outlet gas flow rate was measured by a bubble meter maintained at ambient conditions. The selectivity of ethylene was calculated by Eq. 1

$$S_{C_2H_4} = \frac{[C_2H_4]}{[C_2H_4] + 0.5[CH_4]} \times 100\% \quad (1)$$

Results and Discussion

Catalyst characterization

Surface Area and Pt Dispersion. Table 1 summarizes the BET specific surface areas for ETS-2 and the various catalyst compositions. The as-received commercial ETS-2 filter cake had the highest surface area of all of the samples measured and when this parent material was calcined at 600°C for 4 h, the surface area for the resulting calcined sample dropped by about 60%. Likewise, when platinum was loaded on the surface and calcined at 500°C, the specific surface area of the 1% Pt-ETS-2 catalyst decreased by a comparable amount indicating the presence of platinum does not have a deleterious effect on the thermal stability of the support.

The changes in surface area are likely due to a sintering effect which is seen in an analogous, copper-exchanged ETS-2. The sintering process for Cu-ETS-2 is progressive[40] and converts the anatase at the center of the ETS-2 platelets into highly crystalline rutile. The difference in specific surface area between the parent material and the calcined samples may be linked to this phase transformation.

Unexpectedly, the addition of even a small amount of Zn further reduced the specific surface area of the catalysts. As the Zn content increased, the specific surface area of the catalysts gradually decreased and then leveled off once the Zn content reached 5 wt %. A minor fraction of the reduction in specific surface area can be assigned to the increase in the mass of the ETS-2 particles when the transition metals are added to the surface. The majority of the reduction in surface area is likely due to an effect the transition metals have on the thermal stability of the titanate. The surface area analyses demonstrated a complete lack of porosity for ETS-2 which eliminates pore blockage as a mechanism for the reduction in surface area.

A change in calcination temperature for the 5% Zn 1% Pt-ETS-2 did not create a meaningful difference in surface area. More importantly, the surface area for this catalyst composition is unchanged after being exposed for several hours to the reducing conditions found in the ethane dehydrogenation reaction which suggests that the catalyst is stable toward temperatures in the range of 500°C under both oxidizing and reducing conditions.

Table 1. BET Surface Area for the Catalysts and Parent Material

Catalyst (Support)	Specific Surface Area (m^2/g)
ETS-2 (150°C)	190
ETS-2 (600°C)	69
1% Pt-ETS-2 (500°C)	83
0.5% Zn, 1% Pt-ETS-2 (500°C)	50
1% Zn, 1% Pt-ETS-2 (500°C)	51
2% Zn, 1% Pt-ETS-2 (500°C)	42
5% Zn, 1% Pt-ETS-2 (500°C)	28
5% Zn, 1% Pt-ETS-2 (500°C(T), tested)	29
5% Zn, 1% Pt-ETS-2 (600°C)	24
7.5% Zn, 1% Pt-ETS-2 (500°C)	28

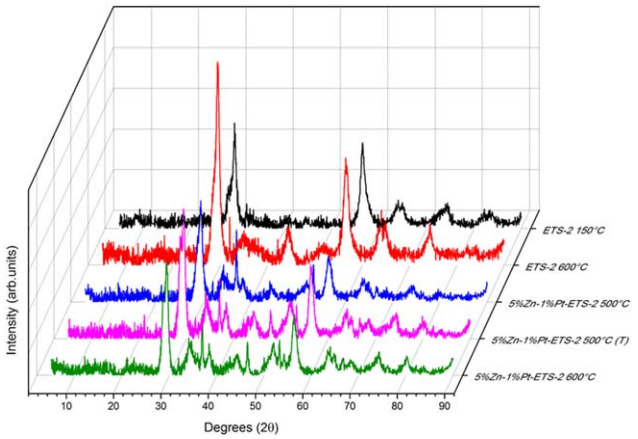

Figure 2. XRD patterns for ETS-2 and 5% Zn 1% Pt-ETS-2.

[Color figure can be viewed in the online issue, which is available at wileyonlinelibrary.com.]

X-ray Diffraction. Figure 2 shows the XRD patterns of the ETS-2 parent material and the catalyst formulation 5% Zn 1% Pt-ETS-2 exposed to different conditions. All of the catalyst compositions were first calcined in air to 500°C for 4 h prior to any subsequent treatment. The broad reflections in the pattern of ETS-2 activated in air at 150°C relate to the anatase phase of TiO_2 and the breadth of the reflections is the result of the nanocrystalline scale of the particles. Upon activation to 600°C, some sharper reflections are evident in the powder pattern. These reflections are due to the progressive phase transition which starts above 550°C[41] that converts the titania in the core of the particles from anatase to rutile. A very broad peak between 32° and 40° 2θ is evident in the sample of the parent material activated to 600°C which does not belong to either the anatase or rutile phase and remains unassigned.

With the addition of zinc and platinum to ETS-2, the powder pattern for the catalyst calcined at 500°C shows two sharp reflections at 37° and 53° 2θ which are not evident in the parent ETS-2 material. These reflections do not correspond to a platinum or zinc oxide/titanate phase but agree well with the (111) and (200) reflections for NaCl. The assignment of these sharp reflections to NaCl is reasonable because the sample was prepared by an incipient wetness technique where the chloride present in the platinate salt remains behind on the solid. The presence of NaCl in the calcined samples suggests that the platinum and/or zinc cations have exchanged with the sodium on the surface of the sodium titanate forming a transition metal-exchanged titanate and NaCl crystallites on the surface of the particles.

A diffraction pattern was collected for a catalyst sample that had completed several hours of ethane dehydrogenation testing at 500°C (5% Zn 1% Pt 500°C(T)). The presence of some additional sharp reflections in the pattern for the sample tested for ethane dehydrogenation (5% Zn 1% Pt 500°C (T)) compared with the same composition only activated in air (5% Zn 1% Pt 500°C) is assigned to the emergence of a larger rutile fraction in this sample. The presence of a larger rutile fraction in the PtZn-ETS-2 500°C (T) sample suggests that the TiO_2 phase transition does proceed at 500°C although the conversion of anatase to rutile must be relatively slow at this temperature. Other than the presence of an incrementally larger rutile fraction, the two diffraction patterns are indistinguishable which indicates that the catalyst support is thermally stable under both oxidative and reductive conditions.

A diffraction pattern was collected on the same catalyst composition calcined in air to 600°C. The diffraction pattern for this sample shows no substantial differences compared with sample calcined at 500°C and contains no reflections that have not already been assigned. This result, in combination with the previous XRD results, indicates that the transition metals remain dispersed on the surface of ETS-2 and do not crystallize into a distinct phase under calcination or test conditions.

Microstructure and Morphology of the Catalysts. Figure 3 shows the images of the catalysts PtZn-ETS-2 and Pt-ETS-2 calcined in air at 600°C for 4 h. Aggregated Pt particles manifest in the back-scatter image (Figure 3a) as bright spots on the surface of the Pt-ETS-2 catalyst. This behavior has previously been seen for silver exchanged on the surface of ETS-2[42] and the assignment of these bright spots as platinum particles was confirmed by higher magnification EDX analysis. Aggregation of active metal component is undesirable due to losses in activity, stability, and selectivity of the catalysts.[9,26] The absence of bright clusters of metal particles on the bimetallic sample (Figure 3b) confirms the effect of zinc as a promoter of platinum dispersion since any metallic particles have been reduced to a size too small to be detected at this resolution. This effect has precedence as zinc has been found to have a similar function for dispersing Pt on alumina.[32,33]

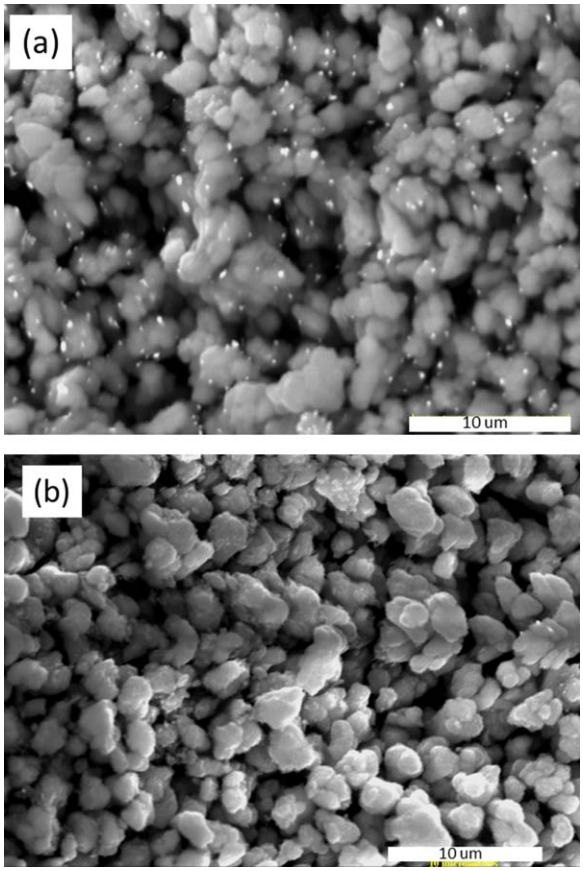

Figure 3. SEM images of (a) 1% Pt-ETS-2 calcined at 600°C and (b) 5% Zn 1% Pt-ETS-2.

[Color figure can be viewed in the online issue, which is available at wileyonlinelibrary.com.]

Interaction of the Promoters and the Support. The 5% Zn 1% Pt-ETS-2 catalyst was calcined in air at either 500°C or 600°C for 4 h and subsequently reduced under 40 vol % H_2 at 40 mL/min and 300°C. The XPS spectra for the reduced samples are shown in Figure 4. When calcined in air at elevated temperatures, the zinc nitrate salt used to prepare the catalysts is expected to decompose to ZnO, which should have a characteristic binding energy of 1022.5 eV.[43,44] The exposure of the oxidized sample to a reducing atmosphere at an elevated temperature should, depending on the thermodynamics, reduce the oxides to their base metals. Zinc metal is, however, difficult to distinguish from ZnO in the XPS spectrum as the binding energies are comparable.

The Zn XPS spectrum for the reduced sample that was calcined at 500°C (Figure 4a) shows only a single peak centered at 1021.3 eV which suggests that the metal remained entirely in its oxidized state or that the ZnO was fully reduced.[44,45] The presence of metallic zinc might be unexpected as thermodynamics suggests that the reduction of ZnO to zinc metal cannot be accomplished efficiently under H_2 using the

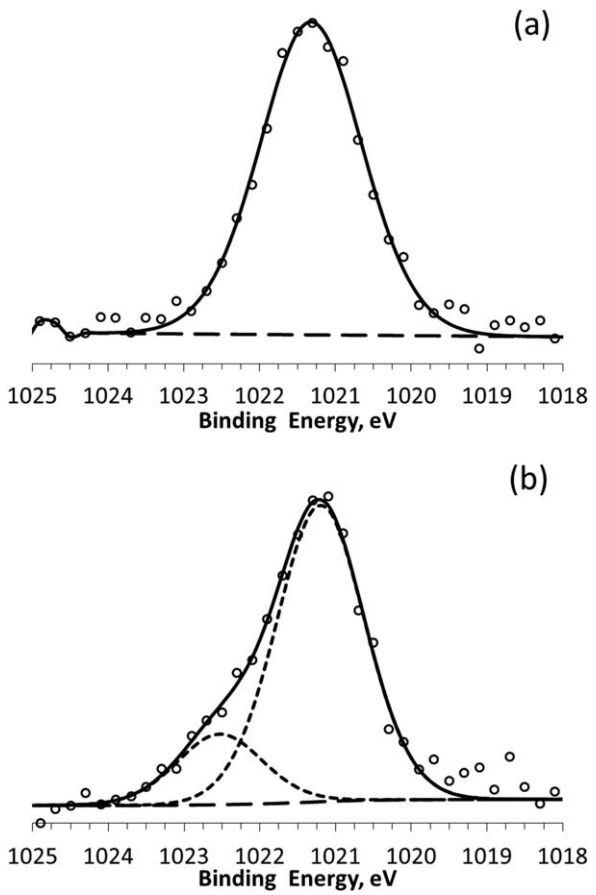

Figure 4. XPS of the Zn $2p_{3/2}$ of the reduced catalyst 5% Zn 1% Pt-ETS-2 calcined (a) at 500°C and (b) at 600°C.

reduction conditions specified because the Gibbs free energy is still positive. The reduction of ZnO under the experimental conditions can, however, take place via a two-step reduction process mediated by platinum. The platinum salt used in preparing the catalyst is easily reduced under the experimental conditions to platinum metal and, once reduced, Pt(0) is exceptionally active toward H_2 dissociation. The hydrogen atoms dissociated on the Pt metal centers can spill over[46–50] to adjacent ZnO species and spontaneously reduce them to their metallic state.

The binding energy for Zn(0) in this sample is lower than the average binding energy of 1021.78 eV expected for both metallic Zn and ZnO. Such a negative shift in the binding energy is generally the result of having increased electron density around the zinc metal center. The core level $2p_{3/2}$ binding energy for the Zn for the catalyst sample calcined at 500°C is likely characteristic of a bimetallic PtZn alloy. The formation of a bimetallic alloy through hydrogen spillover from one transition metal to an adjacent metal oxide has been observed for a Cu/ZnO catalyst used for methanol synthesis.[46,51]

The calcination of the same catalyst formulation in air to 600°C significantly changes the XPS spectrum of the reduced catalyst. The spectrum for the Zn core level $2p_{3/2}$ for this sample can be deconvoluted into two bands centered at 1022.5 and 1021.1 eV. The binding energy 1021.1 eV is similar to that seen for the PtZn alloy seen in the sample calcined at 500°C. A remaining peak, centered on a higher binding energy, implies a portion of the zinc remained in an oxide phase that is resistant to reduction. It is likely that the higher calcination temperature increased the interaction between the titanate framework and the ZnO to form a new oxide phase with the titanate substrate that is resistant to reduction by the hydrogen that spills over from the platinum metal centers. By integrating the two peak areas, it can be calculated that, for the catalyst calcined at 600°C, only 80% of ZnO was reduced to Zn(0) and that the remaining ZnO was too strongly associated with the surface of ETS-2 to be reduced.

The XPS results suggest that when the PtZn-ETS-2 catalyst is calcined at lower temperatures, the ZnO has a weaker interaction with the support which allows it to be more easily reduced by hydrogen that has spilled over from the Pt and promotes intermetallic bonding between zinc and platinum. However, when the catalyst is treated at the higher temperature, a portion of the ZnO reacts with the support to form an oxide phase, which is resistant to reduction. Catalyst evaluations (not shown) demonstrated that the bimetallic PtZn-ETS-2 catalysts treated at 600°C had a lower activity than the same compositions treated at 500°C. As a result, the ethane dehydrogenation results presented here are for reduced catalyst formulations first calcined at 500°C in air.

Temperature Programmed Desorption. The behavior of the Zn and Pt toward reduction can be studied using temperature programmed reduction and is diagnostic toward assessing bimetallic interactions.[52] Figure 5 shows the normalized H_2-TPR profiles of three ETS-2 samples, spanning a range of compositions, all of which had been calcined in air at 500°C. Samples containing only platinum, only zinc, and a single bimetallic composition were tested to examine whether the bimetallic system, as suggested by the XPS analysis, demonstrates any measurable differences compared with the pure component systems.

H_2 consumption is associated with the reduction of the transition metal oxide to its associated metal and the TPR curves reflect the differences in the reduction potential of the different catalyst formulations. The platinum on the 1% Pt-ETS-2 catalyst was easily reduced as the reduction started slightly above

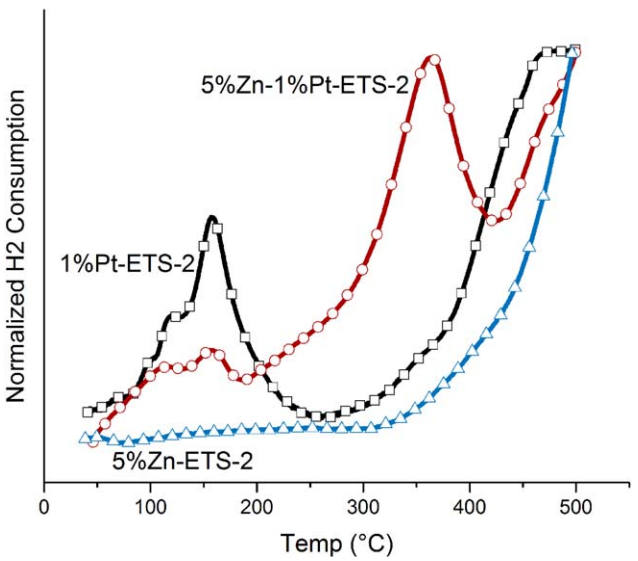

Figure 5. H_2-TPR profiles of ETS-2 supported catalysts.

[Color figure can be viewed in the online issue, which is available at wileyonlinelibrary.com.]

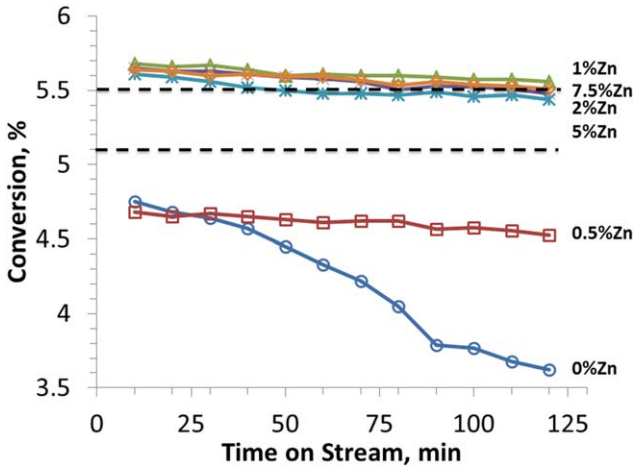

Figure 6. Ethane conversion over 1% Pt-ETS-2 catalysts modified with different Zn contents at 510°C, WHSV = 0.87 h^{-1}.

The dashed lines represent the ideal equilibrium conversion at 510 and 515°C. [Color figure can be viewed in the online issue, which is available at wileyonlinelibrary.com.]

room temperature and continued as the temperature increased until 250°C where the reduction was largely complete. The Zn on 5% Zn-ETS-2, by contrast, did not even begin to reduce until 330°C and the bulk of the reduction took place at much higher temperatures. The bimetallic catalyst, however, has a unique TPR profile. Three reduction peaks are evident for this sample; two at low temperatures and one high temperature. The two low temperature peaks centered at 110 and 130°C agree well with the profile for platinum in 1% Pt-ETS-2 s while the higher temperature peak centered at 360°C is likely due to the reduction of zinc. These results confirm the mechanism of hydrogen spillover and its effect on suppressing the reduction temperature for ZnO. A suppression of the reduction potential of ZnO would not be expected without an interaction between the Zn and Pt on the surface of ETS-2.

The TPR results suggest that reducing the 5% Zn 1% Pt-ETS-2 catalyst to about 400°C should result in the complete reduction of the transition metals. The reducing conditions the catalysts were exposed to in the process of preparing and testing them are different compared with the TPR conditions. While 10% H_2 was used in the TPR study, 40% H_2 was used to reduce the calcined catalysts—although a lower temperature was used (300°C). The absence of a ZnO phase in the XPS results (Figure 4a) suggest that catalyst samples calcined at 500°C and subsequently reduced under the specified experimental conditions yield a fully reduced sample.

Subsequent to reduction, the catalysts are then subjected to pure ethane at ~510°C which provides a lower concentration of H_2 (~5%) but a higher temperature. It is difficult to speculate whether the catalyst undergoes further reduction when subjected to the conditions used for ethane dehydrogenation. Overly aggressive reducing conditions would be expected to sinter the transition metals yet the XRD pattern for the catalyst calcined and tested at 500°C (Figure 2) does not show any evidence of a metallic phase being present in the sample after testing. The XPS and XRD results indicate that the catalyst is suitably stable to the reducing conditions encountered in this study and suggests that the catalysts are fully reduced in 40% H_2 at 300°C and do not undergo further reduction when tested as ethane dehydrogenation catalysts.

Effect of Zn on the activity, selectivity, and stability of ethane dehydrogenation

The conversion and selectivity of the bimetallic PtZn-ETS-2 catalysts toward ethane dehydrogenation was tracked over a period of at least 2 h to ensure that the system was at steady state and to allow for a measurable amount of coke to form on the surface of the catalysts.

The ethane conversion and ethylene selectivity (calculated using Eq. 1) with respect to time for the various catalysts are shown in Figures 6 and 7, respectively. The HSC software package from Outotec.com was used to calculate the ideal conversion of ethane at 510°C (5.1%) and 515°C (5.5%). The temperature of the bed was measured using a thermocouple inserted in the middle of the bed (Figure 1). The placement of the thermocouple may not capture thermal gradients across the bed and it is reasonable to expect, particularly with an endothermic reaction, that outer portion of the bed may be hotter than the center. Being endothermic, the dehydrogenation reaction is highly sensitive to temperature and an uncertainty of even a few degrees can significantly change the expected degree of conversion.

Figure 6 demonstrates that the conversion of ethane over the 1% Pt-ETS-2 catalyst (labeled as 0% Zn) was low and that the activity was not stable over the duration of the measurement. The addition of 0.5% Zn did not significantly improve the conversion although the stability of the catalyst over time was greatly improved. For Zn loadings at and in excess of 1 wt %, the thermodynamic equilibrium values for ethane conversion at the experimental temperature were achieved and all of the samples displayed excellent stability over time. The slight downward trend seen with these samples may be the result of progressive catalyst deactivation or, more likely, is the result of a minor cooling trend in the furnace and/or bed. At 120 min, the measured conversion suggests that the majority of the bed was closer to 515°C rather than the 510°C suggested by the thermocouple.

In Figure 7, it can be seen that the ethylene selectivity increased with time for the 1% Pt-ETS-2 catalyst but consistently remained below 100% due to the constant presence of methane in the product gas (an indicator of undesirable side reactions). The addition of 0.5 wt % Zn to 1% Pt-ETS-2

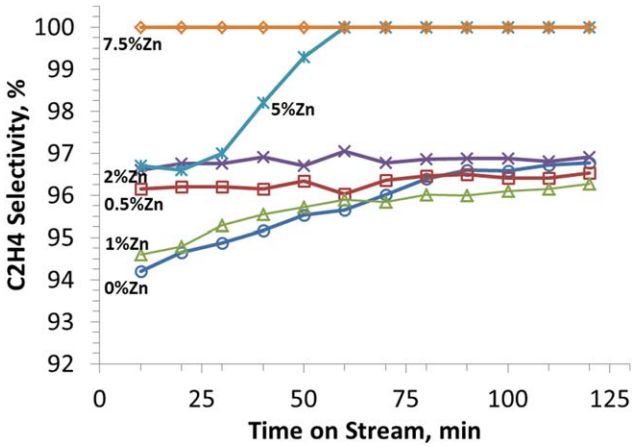

Figure 7. Ethylene selectivity over 1% Pt-ETS-2 catalysts modified with different Zn contents at 510°C, WHSV = 0.87 h^{-1}.

[Color figure can be viewed in the online issue, which is available at wileyonlinelibrary.com.]

provided an improvement in catalyst stability but did not significantly alter the selectivity of the catalyst as side reactions were still present evidenced, again, by CH_4 in the product stream. At Zn loadings of 5% and above, a significant improvement in selectivity is noted which was not necessarily implied from the conversion data in Figure 6. At and above 5% Zn, product stream contained only an equilibrium mixture of ethane, ethylene, and hydrogen. The absence of any measureable concentration of methane suggests the catalysts are wholly selective toward ethylene dehydrogenation. The observation that higher Zn contents not only improved catalyst activity, but significantly increased ethylene selectivity, implies that the Zn is acting as a promoter and, through intermetallic bonding, has changed the electronic properties of active Pt metal phase[31] in such a way as to prevent the formation of methane.

The methane seen in the product stream for several of the catalyst compositions is the main side product of ethane dehydrogenation and isotopic labeling tests have shown that ethylene is the precursor for methane production.[5] Ethylene readsorption is, therefore, the main contribution to methane and coke formation.[7] Yagasaki and Masel[36] found that coke and methane were mainly formed on the (1 × 1)Pt(110) surface by the decomposition of adsorbed ethylene (π-bonded) at elevated temperatures. The key to suppress coke deposits and methane by-product was to prevent the readsorption of ethylene onto the Pt surface.[7] Rodriguez and Kuhn[45] investigated chemical and electronic properties of Pt bimetallic surfaces, and concluded that the formation of PtZn bimetallic bond on Pt(111) surfaces caused the density of Pt 5d electrons to shift to 6s and 6p. Zn has the similar electronic perturbations as early transition metals (Group 3, 4 metals) to Pt, but larger than late transition metals (Group 8–11 metals, by the IUPAC definition). The presence of zinc on the surface of Pt-ETS-2 causes electronic perturbations in the Pt which weakens the strength of the Pt(5d) π-bonding interactions, and subsequently reduces the ability of the Pt to chemisorb ethylene and hence cause side reactions. The contribution of electron density from the platinum π-bonding orbital to zinc is supported by the XPS results which showed an decrease in the binding energy of the $2p_{3/2}$ electrons for Zn(0). The ability of Zn to suppress readsorption of ethylene is augmented by the open surface characteristics of ETS-2 which, lacking any pore structure, cannot concentrate the cracked products into micropores or hinder the desorption of cracked products. The intrinsic properties of the PtZn catalyst system coupled with the nonporous architecture of ETS-2 allows for virtually complete selectivity for ethane dehydrogenation for several bimetallic compositions.

To confirm that the methane observed with some of the catalyst formulations was due to conventional ethane dehydrogenation side reactions—which are known to produce coke—TG-MS was employed to study the combustion products liberated from spent samples of catalyst. The TG-MS traces of the spent 1% Zn 1% Pt-ETS-2 and 5% Zn 1% Pt-ETS-2 catalysts are shown in Figure 8. Prior to the TG-MS measurements, both catalysts were exposed to a continuous flow of ethane at 600°C for about 4 h. The higher temperature was selected to increase the degree of ethane conversion and to accelerate the rate of coke formation on the surface of the catalyst.

For the catalyst with 5 wt % Zn, the weight loss out to 600°C was only 2.2 wt % and the absence of any signal above

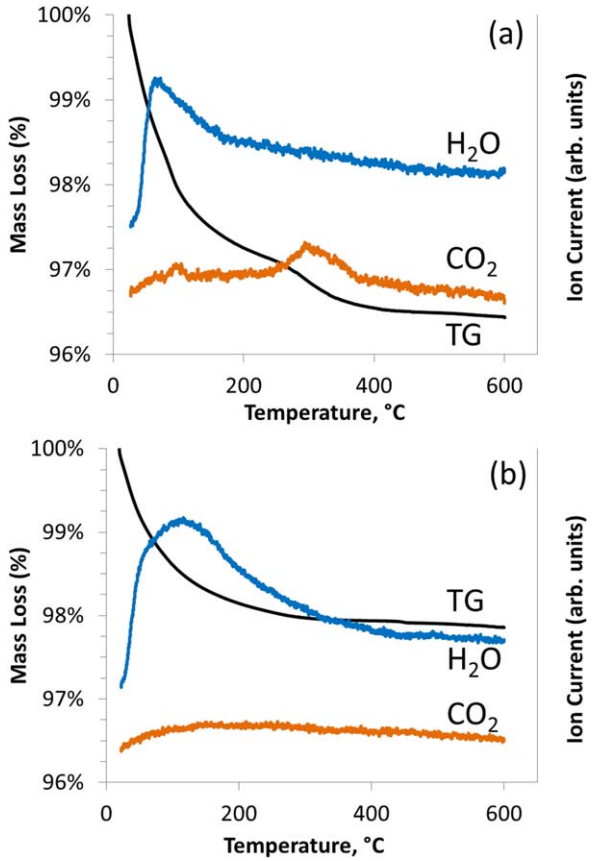

Figure 8. TG-MS analysis of catalysts (a) 1% Zn-1% Pt-ETS-2 and (b) 5% Zn-1% Pt-ETS-2 tested at 600°C.

[Color figure can be viewed in the online issue, which is available at wileyonlinelibrary.com.]

baseline for the CO_2 fragment in the MS trace establishes that all the weight loss was associated with water that was either physically adsorbed on the surface or present as hydroxyl groups terminating the surface of the titanate particles. For the 1 wt % Zn catalyst, however, a CO_2 peak centered at 300°C is evident in the MS trace. The combustion of coke at such temperatures is reasonable as the coke was deposited at a relatively low temperature compared with the higher temperature, thermal cracking process which forms more graphitic coke. The MS trace confirms the presence of coke on the surface of the catalyst and confirms that conventional side reactions were responsible for the observed reduction in catalyst selectivity. The amount of total weight loss for the 1% Zn sample was 3.6 wt % which suggests a coke content of about 1.5 wt %. While the product gas composition was not measured, the absence of coke on the 5% Zn catalyst suggests catalysts having higher Zn loadings maintain their selectivity at temperatures as high as 600°C.

An unexpected sensitivity was found when the conversion and selectivity of the various catalysts was measured as a function of the weight hourly space velocities (WHSV) of the reactant gas. The results of this study are summarized in Figure 9. The conversion and selectivity for the catalysts containing less than 5% Zn are profoundly affected by increasing the space velocity of the ethane feed gas. At lower velocity, a Zn loading of 5 wt % was necessary to achieve complete conversion and selectivity but by increasing the space velocity of the

feed gas by a factor of 1.3, catalyst compositions as low as 1% Zn are able to achieve complete conversion and selectivity. At the higher velocity, catalysts containing Zn loadings from 1 to 7.5 wt % were all equally capable of generating an equilibrium mixture of ethane, ethylene, and hydrogen without any measurable side reaction.

The effect of the feed rate on the conversion and selectivity was studied across a wider range of velocities for two catalyst compositions and the results are shown in Figure 10. For the 2% Zn catalyst (Figure 10a), a step change is evident at around WHSV = 1.1 after which the ethylene selectivity is maximized. The selectivity of the 5% Zn sample (Figure 10b) shows no sensitivity to the space velocity of the reactant gas and the selectivity of the catalyst remains flat across the entire range tested. Even at low space velocities, the 5% Zn composition generates an equilibrium mixture of ethane, ethylene, and hydrogen in the absence of any measurable side reactions.

The ethane conversion for both catalysts decreases with respect to WHSV which might suggest that the gas is not reaching equilibrium over the catalyst as the feed velocity increases. The selectivity for the 5% Zn catalyst, however, remains unchanged across the entire range of velocities tested which suggests that the catalyst is not significantly influenced by the space velocity of the feed gas. The monotonic decrease in ethane conversion as a function of WHSV is similar for

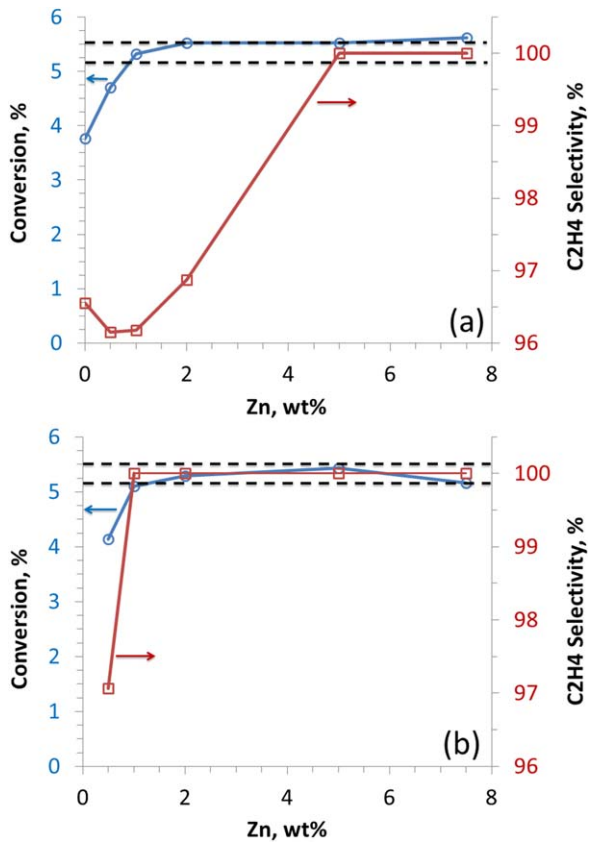

Figure 9. Effects of Zn content on 1% Pt-ETS-2 catalyst on conversation and selectivity at (a) WHSV = 0.87 h^{-1} and (b) WHSV = 1.14 h^{-1} at 510°C.

The dashed lines represent the ideal equilibrium conversion at 510 and 515°C. [Color figure can be viewed in the online issue, which is available at wileyonlinelibrary.com.]

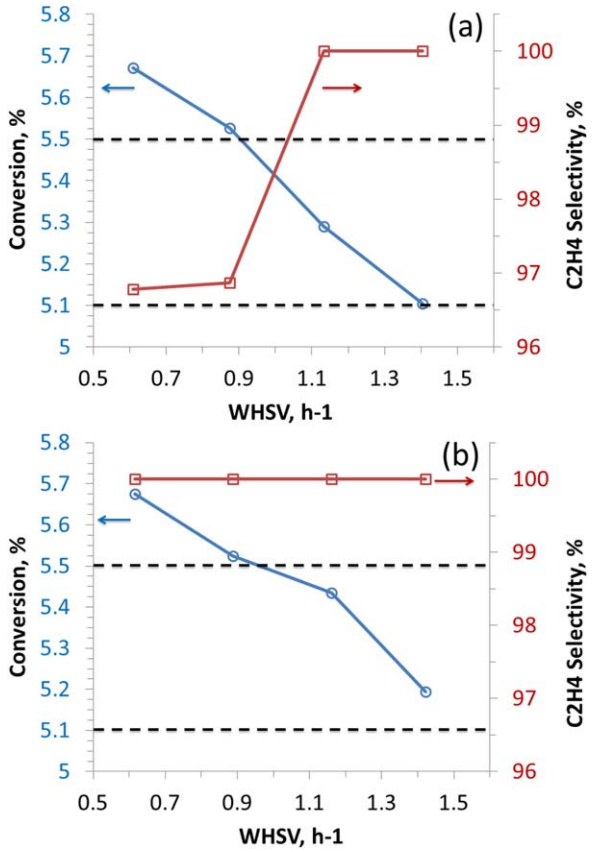

Figure 10. Effects of WHSV on conversion and selectivity with (a) 2% Zn-1% Pt-ETS-2 and (b) 5% Zn-1% Pt-ETS-2 catalysts at 510°C.

The dashed lines represent the ideal equilibrium conversion at 510 and 515°C. [Color figure can be viewed in the online issue, which is available at wileyonlinelibrary.com.]

both catalysts which was unexpected for catalysts having measurably different ethylene selectivities with respect to the same variable. The trend for ethane conversion is more likely due to a cooling trend in the bed brought about by the greater mass flow of gas into the catalyst bed. The reactor system shown in Figure 1 was not specifically designed to preheat the higher gas flows and it is reasonable to assume that the gas enters the catalyst bed at a progressively lower temperature as the gas velocity is increased. The cooling effect of the gas needs only to be about 5°C to explain the trend seen in Figure 10.

Conclusions

The combination of Zn with Pt on the surface of the titanate ETS-2 generates a catalyst capable of complete selectivity at steady state for a range of bimetallic compositions and across a range of space velocities. The platinum acts on the Zn to reduce it at a much lower temperature than predicted by thermodynamics due to the formation of hydrogen ions over the platinum metal centers. The zinc metal subsequently interacts with the Pt through intermetallic bonding to mute the tendency Pt has to readsorb ethylene and subsequently produce methane and coke.

Acknowledgments

This work was generously supported by NOVA Chemicals Corporation. Support from the Natural Sciences and Engineering Research Council Industrial Research Chair in Molecular Sieve Separations Technology is also gratefully acknowledged.

Literature Cited

1. Bewley L. IHS WPC 2012: shale reshapes ethylene markets. *Chem Week*. 2012;174(10):15.
2. Holmquist K. Global ethylene surplus to last through 2011. *Oil Gas J*. 2010;108(27):46–52.
3. Zimmermann H, Walzl R. Ethylene. *Ullmann's Encyclopedia of Industrial Chemistry, Vol. 13, 6th ed*. Germany: Wiley-VCH Verlag GmbH & Co. KGaA, 2009:465–529.
4. Vincent RS, Lindstedt RP, Malik NA, Reid IAB, Messenger BE. The chemistry of ethane dehydrogenation over a supported platinum catalyst. *J Catal*. 2008;260(1):37–64.
5. Virnovskaia A, Rytter E, Olsbye U. Kinetic and isotopic study of ethane dehydrogenation over a semicommercial Pt,Sn/Mg(Al)O catalyst. *Ind Eng Chem Res*. 2008;47(19):7167–7177.
6. Yokoyama C, Bharadwaj SS, Schmidt LD. Platinum-tin and platinum-copper catalysts for autothermal oxidative dehydrogenation of ethane to ethylene. *Catal Lett*. 1996;38(3–4):181–188.
7. Galvita V, Siddiqi G, Sun P, Bell AT. Ethane dehydrogenation on Pt/Mg(Al)O and PtSn/Mg(Al)O catalysts. *J Catal*. 2010;271(2):209–219.
8. Sun P, Siddiqi G, Vining WC, Chi M, Bell AT. Novel Pt/Mg(In)(Al)O catalysts for ethane and propane dehydrogenation. *J Catal*. 2011;282(1):165–174.
9. Wu J, Peng ZM, Bell AT. Effects of composition and metal particle size on ethane dehydrogenation over PtxSn100-x/Mg(Al)O (70 <= x <= 100). *J Catal*. 2014;311:161–168.
10. Bandiera J, BenTaarit Y. Ethane conversion: kinetic evidence for the competition of consecutive steps for the same active centre. *Appl Catal A Gen*. 1997;152(1):43–51.
11. Caeiro G, Carvalho RH, Wang X, Lemos MANDA, Lemos F, Guisnet M, Ramôa Ribeiro F. Activation of C2–C4 alkanes over acid and bifunctional zeolite catalysts. *J Mol Catal A Chem*. 2006;255(1–2):131–158.
12. Cortright RD, Hill JM, Dumesic JA. Selective dehydrogenation of isobutane over supported Pt/Sn catalysts. *Catal Today*. 2000;55(3):213–223.
13. Akporiaye D, Jensen SF, Olsbye U, Rohr F, Rytter E, Rønnekleiv M, Spjelkavik AI. A novel, highly efficient catalyst for propane dehydrogenation. *Ind Eng Chem Res*. 2001;40(22):4741–4748.
14. Tsyganok A, Harlick PJE, Sayari A. Non-oxidative conversion of ethane to ethylene over transition metals supported on Mg–Al mixed oxide: preliminary screening of catalytic activity and coking ability. *Catal Commun*. 2007;8(5):850–854.
15. Siddiqi G, Sun PP, Galvita V, Bell AT. Catalyst performance of novel Pt/Mg(Ga)(Al)O catalysts for alkane dehydrogenation. *J Catal*. 2010;274(2):200–206.
16. Wu J, Peng Z, Sun P, Bell AT. n-Butane dehydrogenation over Pt/Mg(In)(Al)O. *Appl Catal A Gen*. 2014;470:208–214.
17. de Miguel S, Castro A, Scelza O, Fierro J, Soria J. FTIR and XPS study of supported PtSn catalysts used for light paraffins dehydrogenation. *Catal Lett*. 1996;36(3–4):201–206.
18. Yu J, Ge Q, Fang W, Xu H. Influences of calcination temperature on the efficiency of CaO promotion over CaO modified Pt/γ-Al2O3 catalyst. *Appl Catal A Gen*. 2011;395(1–2):114–119.
19. de Graaf EA, Rothenberg G, Kooyman PJ, Andreini A, Bliek A. Pt0.02Sn0.003Mg0.06 on γ-alumina: a stable catalyst for oxidative dehydrogenation of ethane. *Appl Catal A Gen*. 2005;278(2):187–194.
20. Nagaraja BM, Jung H, Yang DR, Jung K-D. Effect of potassium addition on bimetallic PtSn supported θ-Al2O3 catalyst for *n*-butane dehydrogenation to olefins. *Catal Today*. 2014;232:40–52.
21. Ballarini AD, de Miguel SR, Castro AA, Scelza OA. *n*-Decane dehydrogenation on Pt, PtSn and PtGe supported on spinels prepared by different methods of synthesis. *Appl Catal A Gen*. 2013;467:235–245.
22. Salmones J, Wang J-A, Galicia JA, Aguilar-Rios G. H2 reduction behaviors and catalytic performance of bimetallic tin-modified platinum catalysts for propane dehydrogenation. *J Mol Catal A Chem*. 2002;184(1–2):203–213.
23. Håkonsen SF, Walmsley JC, Holmen A. Ethene production by oxidative dehydrogenation of ethane at short contact times over Pt-Sn coated monoliths. *Appl Catal A Gen*. 2010;378(1):1–10.
24. Iglesias-Juez A, Beale AM, Maaijen K, Weng TC, Glatzel P, Weckhuysen BM. A combined in situ time-resolved UV–Vis, Raman and high-energy resolution X-ray absorption spectroscopy study on the deactivation behavior of Pt and PtSn propane dehydrogenation catalysts under industrial reaction conditions. *J Catal*. 2010;276(2):268–279.
25. Nawaz Z, Wei F. Hydrothermal study of Pt–Sn-based SAPO-34 supported novel catalyst used for selective propane dehydrogenation to propylene. *J Ind Eng Chem*. 2010;16(5):774–784.
26. Vu BK, Song MB, Ahn IY, Suh Y-W, Suh DJ, Kim W-I, Koh H-L, Choi YG, Shin EW. Pt–Sn alloy phases and coke mobility over Pt–Sn/Al2O3 and Pt–Sn/ZnAl2O4 catalysts for propane dehydrogenation. *Appl Catal A Gen*. 2011;400(1–2):25–33.
27. Vu BK, Song MB, Ahn IY, Suh Y-W, Suh DJ, Kim W-I, Koh H-L, Choi YG, Shin EW. Propane dehydrogenation over Pt–Sn/Rare-earth-doped Al_2O_3: influence of La, Ce, or Y on the formation and stability of Pt–Sn alloys. *Catal Today*. 2011;164(1):214–220.
28. Hauser AW, Gomes J, Bajdich M, Head-Gordon M, Bell AT. Subnanometer-sized Pt/Sn alloy cluster catalysts for the dehydrogenation of linear alkanes. *Phys Chem Chem Phys*. 2013;15(47):20727–20734.
29. Nagaraja BM, Shin C-H, Jung K-D. Selective and stable bimetallic PtSn/θ-Al_2O_3 catalyst for dehydrogenation of n-butane to *n*-butenes. *Appl Catal A Gen*. 2013;467:211–223.
30. Candy JP, Roisin E, Basset JM, Uzio D, Morin S, Fischer L, Olivier-Fourcade J, Jumas JC. Evidence for direct observation by Mossbauer spectroscopy of surface tin atoms in platinum-tin particles. *Hyperfine Interact*. 2005;165(1–4):55–60.
31. Yu CL, Xu HY, Ge QJ, Li WZ. Properties of the metallic phase of zinc-doped platinum catalysts for propane dehydrogenation. *J Mol Catal A Chem*. 2007;266(1–2):80–87.
32. Zhang YW, Zhou YW, Shi JJ, Sheng XL, Duan YZ, Zhou SJ, Zhang ZW. Effect of zinc addition on catalytic properties of PtSnK/gamma-Al_2O_3 catalyst for isobutane dehydrogenation. *Fuel Process Technol*. 2012;96:220–227.
33. Wang YJ, Wang YM, Wang SR, Guo XZ, Zhang SM, Huang WP, Wu SH. Propane dehydrogenation over PtSn catalysts supported on ZnO-modified $MgAl_2O_4$. *Catal Lett*. 2009;132(3–4):472–479.
34. Silvestre-Albero J, Serrano-Ruiz JC, Sepulveda-Escribano A, Rodriguez-Reinoso F. Modification of the catalytic behaviour of platinum by zinc in crotonaldehyde hydrogenation and iso-butane dehydrogenation. *Appl Catal A Gen*. 2005;292:244–251.
35. Bosch P, Valenzuela MA, Zapata B, Acosta D, Aguilarrios G, Maldonado C, Schifter I. High-temperature treated Pt/Sn-$ZnAl_2O_4$ catalysts. *J Mol Catal*. 1994;93(1):67–78.
36. Yagasaki E, Masel RI. Ethylene adsorption and decomposition on (1 $\times$ 1) Pt(110): chemistry of the coke formation site on platinum? *Surf Sci*. 1989;222(2–3):430–450.
37. Ohta M, Ikeda Y, Igarashi A. Additive effect on properties of Pt/ZnO catalyst for dehydrogenation of isobutane at low temperatures. *J Jpn Petrol Inst*. 2002;45(3):150–155.
38. Ohta M, Ikeda Y, Igarashi A. The properties of Pt/ZnO catalyst for dehydrogenation of isobutane at low temperatures. *J Jpn Petrol Inst*. 2002;45(3):144–149.
39. Kuznicki SM. Large-pored crystalline titanium molecular sieve zeolites. 1987, US Patent 5,011,591.
40. Rezaei S, Tavana A, Sawada J, Wu L, Junaid A, Kuznicki S. Novel copper-exchanged titanosilicate adsorbent for low temperature H_2S removal. *Ind Eng Chem Res*. 2012;51:12430–12434.
41. Yazdanbakhsh F, Bläsing M, Sawada JA, Rezaei S, Müller M, Baumann S, Kuznicki SM. Copper exchanged nanotitanate for high temperature H_2S adsorption. *Ind Eng Chem Res*. 2014;53:11734–11739.
42. Shi M, Lin C, Wu L, Holt C, Mitlin D, Kuznicki S. Nanosilver particle formation on a high surface area titanate. *J Nanosci Nanotechnol*. 2010;10:8448–8451.
43. Gaarenstroom SW, Winograd N. Initial and final state effects in the ESCA spectra of cadmium and silver oxides. *J Chem Phys*. 1977;67(8):3500–3506.
44. Silvestre-Albero J, Sepúlveda-Escribano A, Rodríguez-Reinoso F, Anderson JA. Influence of Zn on the characteristics and catalytic behavior of TiO_2-supported Pt catalysts. *J Catal*. 2004;223(1):179–190.
45. Rodriguez JA, Kuhn M. Chemical and electronic properties of Pt in bimetallic surfaces: photoemission and CO-chemisorption studies for Zn/Pt(111). *J Chem Phys*. 1995;102(10):4279–4289.
46. Prins R. Hydrogen spillover. Facts and fiction. *Chem Rev*. 2012;112(5):2714–2738.

47. Rozanov VV, Krylov OV. Hydrogen spillover in heterogeneous catalysis. *Russ Chem Rev*. 1997;66(2):107–119.
48. Roland U, Salzer R, Braunschweig T, Roessner F, Winkler H. Investigations on hydrogen spillover. Part 1. Electrical conductivity studies on titanium dioxide. *J Chem Soc Faraday Trans*. 1995;91(7):1091–1095.
49. Conner WC, Falconer JL. Spillover in heterogeneous catalysis. *Chem Rev*. 1995;95(3):759–788.
50. Sermon PA, Bond GC. Hydrogen spillover. *Catal Rev Sci Eng*. 1974;8(1):211–239.
51. Nakamura J, Choi Y, Fujitani T. On the issue of the active site adn role of ZnO in Cu/ZnO methanol synthesis catalyst. *Top Catal*. 2003;22(3–4):277–285.
52. Padro C, de Miguel S, Castro A, Scelza O. Stability and regeneration of supported PtSn catalysts for propane dehydrogenation. *Studies Surf Sci Catal*. 1997;111:191–198.

Manuscript received Apr. 24, 2015, and revision received June 24, 2015.